ISBN: 978-3-95450-191-5 doi:10.18429/JACoW-SRF2017-MOPB004

DESIGN OF A RF QUADRUPOLE RESONATOR FOR LANDAU DAMPING IN HL-LHC

K. Papke* and A. Grudiev, CERN, Geneva, Switzerland

Abstract

The design and optimization of a quadrupole resonator for transverse Landau damping in the High Luminosity Large Hadron Collider (HL-LHC) is presented. Two different cavity types are considered whose shape is determined by the quadrupolar strength, surface peak fields, and beam coupling impedance. The lower order and higher order mode spectra of the optimized cavities are investigated and different approaches for their damping are proposed. Furthermore, the required RF power and optimal external quality factor for the input coupler are derived.

INTRODUCTION

The betatron frequency spread in circular accelerators yield a natural effect of suppressing transverse collective instabilities, the so-called Landau damping [1]. The incoherent frequency or tune spread is caused by non-linearities in the machine. To ensure this mechanism dedicated nonlinear elements, typically octupole magnets, also known as Landau Octupoles (LO) are installed in the accelerator [2]. However, adiabatic damping and increased beam rigidity reduce their efficiency at higher energies. Future accelerators may call for more efficient devices in order to satisfy the beam requirements at higher energies.

Recently in [3], a superconducting RF quadrupole resonator was proposed as an alternative to the LOs. Its performance is affected likewise by beam rigidity but not by the adiabatic damping since in contrast to magnets, a RF quadrupole resonator introduces a longitudinal instead of a transverse betatron tune spread. The stabilization mechanism of a quadrupole resonator has been proven experimentally by using Q'' which likewise introduces a longitudinal betatron tune spread [4].

The variation of the betatron frequency due to quadrupolar focusing (so-called detuning) is proportional to the integrated quadrupolar strength b_2 which again is correlated to the transverse kick $\Delta\mathbf{p}_\perp^i$ that a particle i experiences while traversing the cavity (Fig. 1).

In [3], it has been demonstrated that an RF quadrupole resonator can result in a significantly more compact solution than a comparable set of octupole magnets providing the same tune spread. In this paper we present the first detailed design and optimization studies of a RF quadrupole resonator for Landau damping based on two types of cavities: the elliptical and the so-called four-vane cavity whose cross sections are shown in Fig. 1.

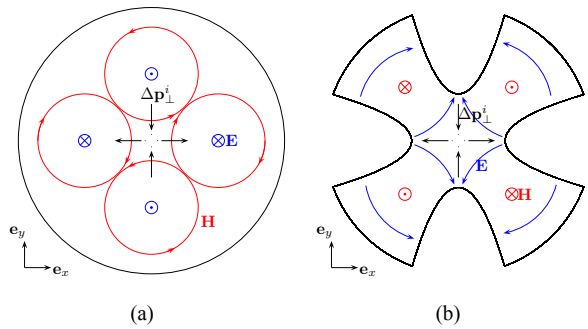

Figure 1: Cross section of quadrupolar field profiles providing the transverse kick to the particle. The force directions corresponds to a negative charge. a) Pillbox with TM-type mode. b) Four-Vane-Cavity with TE-type mode.

CAVITY DESIGN PARAMETERS

The parameters used to optimize the SC cavity can be differentiated into two categories. First, parameters that are derived from eigenmode simulations such as b_2 and second, parameters derived from wakefield simulations such as the transverse and longitudinal impedance. The latter is considerably more time-consuming than eigenmode calculations, hence, it is desirable to minimize the number of wakefield simulations. We propose, first, to optimize the designs independently of the impedance but with varying aperture which has the main influence on the impedance and, second, to calculate the impedance as a subsequent step for each pre-optimized design.

Integrated Quadrupolar Strength b_2

The integrated quadrupolar strength b_2 [5] should be as high as possible to minimize the total number of cavities. The values shown in Table 1 provide an equivalent stabilization effect as the LOs in HL-LHC at a specific chromaticity [6]. They are obtained from macro particle tracking simulation comprising 6×10^5 turns. Though only for a specific case of instability, we use these results as a reference for the cavity design in this paper.

* kai.papke@cern.ch

ISBN: 978-3-95450-191-5 doi:10.18429/JACoW-SRF2017-MOPB004

Table 1: Required b_2 Yielding the Same Stabilization as Provided by LOs for HL-LHC at a chromaticity $Q'_{x,y}$=10 [6]

Frequency [MHz]	b_2 [Tm/m]
400	0.35
800	0.27
1200	0.40

Frequency

The maximum coherent tune shift the quadrupole resonator is able to stabilize by Landau damping depends on the frequency as the curvature of the cosine wave along the bunch introduce the non-linearity. The frequency is limited to harmonics of the main RF system (e.g. for LHC 400, 800 or 1200 MHz). According to the results shown in Table 1, a frequency of 800 MHz is favored which is consistent with [3].

Field Limitation

The strength is limited by either the peak magnetic or electric surface field. Therefore, it is reasonable to maximize the quantities b_2/B_{pk} and b_2/E_{pk} while a ratio $B_{pk}/E_{pk} = 2.13\,\mathrm{mT}/(\mathrm{MV/m})$ represents a good balance between both, the electric and magnetic surface peak fields with respect to the current technical limitations [7].

Impedance

The limited impedance budget guaranteeing a stable beam operation in the accelerator asks for a minimized narrow and broadband impedance. We use the definition from [8] to quantify the effective longitudinal and transverse impedance of the quadrupole resonator denoted as $(Z_\parallel/n)_{\mathrm{eff}}$ and $(Z_\perp)_{\mathrm{eff}}$. All impedance calculations assume a bunch length with RMS sigma of $\sigma_z = 80\,\mathrm{mm}$. The total effective impedance of the required quadrupole resonators for LHC should be far below the limits shown in Table 2.

Table 2: Impedance Budget for LHC [8]

Parameter	Value
$(Z_\parallel/n)_{\mathrm{eff}}$	93 mΩ
$(Z_\perp)_{\mathrm{eff}}$	20 MΩ

Mechanical Restrictions

Finally, a few mechanical limitations should be mentioned:

- The minimal aperture is 20 mm.
- Due to the bending process of niobium sheet, the minimal curvature radius is 10 mm.
- The maximum length of the entire system including the cryomodule(s) is 10 m (LHC layout constraint).

ELLIPTICAL CAVITY

The standard non-reentrant elliptic cavity provides a good reference for other cavity types which are typically more complicated to fabricate [Fig. 2(a)]. In the frame of the optimizations, we observed a correlation between the optimal transition angle α (common tangential angle of both ellipses and the straight part) and b_2 that motivated the extension of the analyses towards reentrant profiles [Fig. 2(b)]. Depending on the iris radius r_{ir}, either a non-reentrant or a reentrant elliptical cavity provides the higher quadrupolar kick.

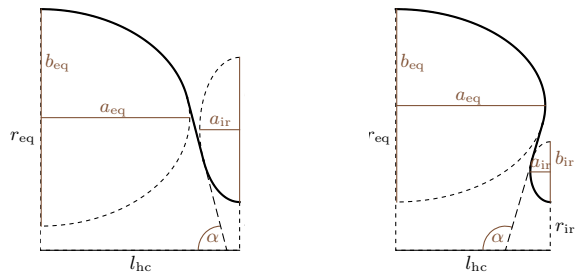

(a) (b)

Figure 2: Profile of elliptical half cells with equator radius r_{eq}, iris radius r_{ir} and length l_{hc}. The dotted lines subscribe the corresponding ellipses as well as the connecting straight with the concerted tangential angle α. (a) Non-reentrant cavity ($\alpha < 90\,\mathrm{deg}$) and (b) reentrant cavity ($\alpha > 90\,\mathrm{deg}$).

It is obvious to choose either the TM_{210} or the TE_{211} mode, both, resulting in the quadrupolar field distributions as qualitatively shown in Fig. 1. However, the latter achieves approximately 40 % less quadrupolar strength for the same amount of stored energy in the cavity due to its longitudinal dependency. Therefore we focus our considerations on the TM_{210} (Fig. 3).

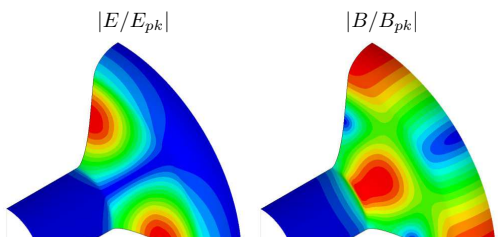

Figure 3: The fields distribution of the TM_{210} mode.

Optimization

The prime objective that defines the "best" cavity shape is given by the maximum possible quadrupolar strength b_2 with respect to the limiting surface peak fields (either B_{pk} or E_{pk}). Throughout all considered designs provided a limitation by the magnetic field ($B_{pk}/E_{pk} > 2.13$). A further major constraint is given by the frequency, typically adjusted via the equator radius r_{eq}. Likewise, the iris radius

ISBN: 978-3-95450-191-5 doi:10.18429/JACoW-SRF2017-MOPB004

is not a free parameter for the optimization because the quadrupolar strength b_2 monotonously increase with decreasing cavity aperture. Instead, we optimize several designs with varying iris radius and subsequently investigate their impedance. The remaining free parameter shown in Fig. 2 have been optimized using a constrained BFGS algorithm[1] together with SLANS2 [9] as 2D eigenmode solver. The implementation is largely parallel allowing a very efficient optimization of even more than five parameters.

The optimizations was carried out with varying iris radii r_{ir} between $25-60\,\mathrm{mm}$ for the reentrant cavities and between $50-175\,\mathrm{mm}$ for the non-reentrant cavities. The transition between both cavity types appears at $r_{\mathrm{ir}}=60\,\mathrm{mm}$ (Fig. 4). The properties of the designs are summarized

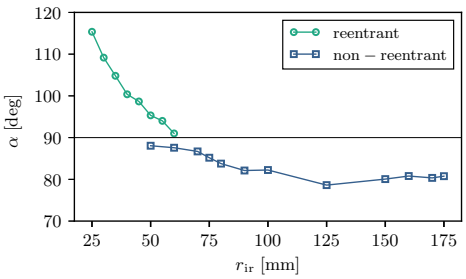

Figure 4: Optimal tangential angle versus the iris radius r_{ir}.

in Figs. 5 and 6. Reentrant elliptical cavities provide a maximum of $b_2=0.16\,\mathrm{Tm/m}$ for the smallest apertures while their counterpart do not achieves more than $b_2=0.12\,\mathrm{Tm/m}$. With increasing aperture the number of required cavities to provide the same betatron tune spread increases monotonically, and thereby the length and impedance of the whole system. Due to a limited space of $10\,\mathrm{m}$ length for HL-LHC and due to economic reasons, the iris radius of the elliptical cavity must not be greater than $r_{\mathrm{ir}}=125\,\mathrm{mm}$.

[1]Broyden Fletcher Goldfarb Shanno algorithm, a group of hill-climbing optimization techniques.

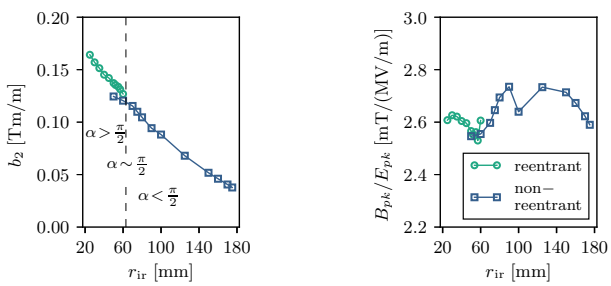

(a) (b)

Figure 5: (a) Quadrupolar strength of the optimized cavities distinguished by their aperture r_{ir} assuming a magnetic peak field at the surface of $B_{pk}=100\mathrm{mT}$. (b) The corresponding ratio of the surface peak fields.

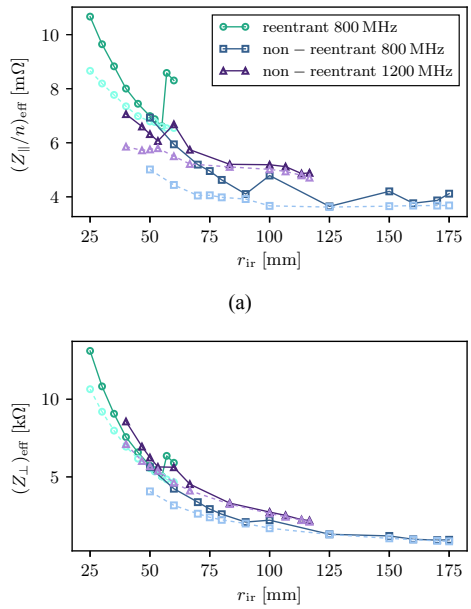

(a) (b)

Figure 6: Effective longitudinal (a) and transverse (b) impedance accumulated over the number of required cavities to satisfy the conditions in Table 1. In solid, the number of cavities is rounded up while in dashed not.

A system of non-reentrant 800MHz elliptical cavities that satisfy the requirements of Table 1 provides an effective longitudinal impedance of at least 4mΩ, almost 5% of the entire LHC impedance budget (Fig. 6). Reentrant cavities provide more than 8% of the budget. The effective transverse impedance [Fig. 6(b)] is not of concern since the results are throughout marginal against the given impedance value in Table 2.

LOMs and HOMs

The potentially harmfull lower and higher order modes (LOMs and HOMs) are listed in Table 3 for an optimized cavity with $r_{\mathrm{ir}}=90\,\mathrm{mm}$. Taking advantage of the field distribution of the quadrupole mode, it is reasonable to extract their power by placing couplers around the equator where the fundamental mode vanishes (Fig. 7). The ports can have a diameter up to 100mm without notably modifying the field distribution or enhancing the surface field.

Table 3: Trapped Lower and Higher Order Modes for a 800 MHz Non-reentrant Elliptical Cavity with r_{ir}=90mm

Mode	f [MHz]	Mode	f [MHz]
TM_{010}	417.7	TM_{110}	594.5
TM_{020}	896.2	TE_{111}	778.2
TE_{011}	1107.5	TE_{121}	1281.0
TM_{011}	1137.9	TM_{131}	1586.7
TE_{021}	1430.9		

ISBN: 978-3-95450-191-5 doi:10.18429/JACoW-SRF2017-MOPB004

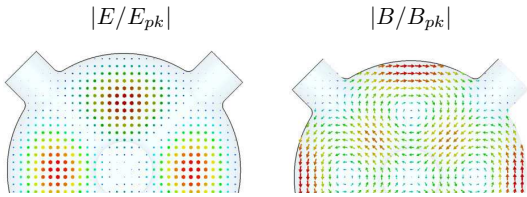

Figure 7: Electric and magnetic field distribution of the quadrupole mode in the transverse plane. The cavity is equipped with ports at the low field regions.

These ports serve also for detuning the other polarization of the TM210 mode.

FOUR-VANE CAVITY

The disadvantages of the previously discussed elliptical cavities can be summarized as follows:

- The maximum achievable b_2 is relatively low.
- The large cavity size ($r_{eq} \sim 300\,\mathrm{mm}$).
- The limitation by the B-field may cause quenching.
- The high effective longitudinal impedance.

All these drawbacks can be resolved by a cavity design whose contour in the transverse plane forms a quadrupole-like electric field [Fig. 1(b)]. The actual cavity is obtained by a smooth transition from the quadrupolar contour to the beam pipe (Figs. 8 and 9). As for the elliptical cavity, we define the transverse contour by two conjugated arcs connected with a straight line. The transition from the quadrupolar contour to the circular beam pipe is defined by the tapering angle α_{tap} .

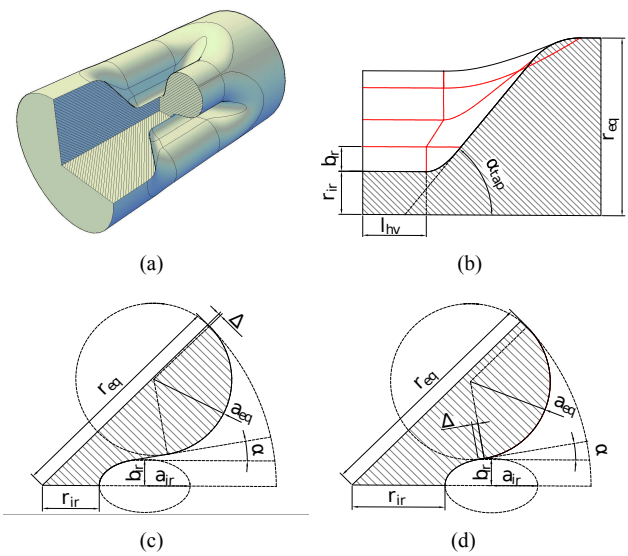

Figure 8: Four-vane cavity design. (a) 3D view of the cavity. (b) Quarter of the longitudinal cross-section. (c) and (d) Two versions of the transverse cross-section (only an eighth). The beam is located along the bottom line in (b) or at the lower left corner in (c) and (d), respectively.

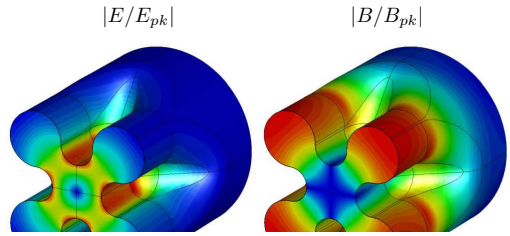

Figure 9: Field distribution of the quadrupole mode.

Optimization

The optimization of the four-vane shape relies on 3D eigenmode solvers using HFSS or CST MWS. A parametric model has been developed for both codes with the difficulty of ensuring a correct construction for any reasonable ensemble of design parameters. The optimization was carried out in a brute force manner with subsequent interpolations applied on the results of numerous parameter sweeps.

The properties of the optimized designs are summarized in Fig. 10 for various apertures (iris radius r_{ir}) and tapering angles α_{tap}. Depending on its aperture a four-vane cavity is able to provide between two to five times more quadrupolar strength than a non-reentrant elliptical cavity with an

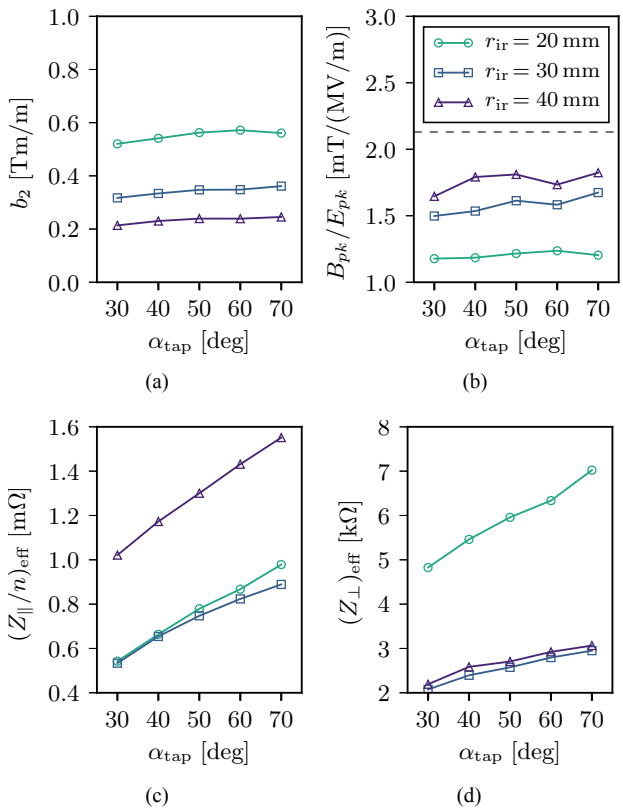

Figure 10: (a) Maximum quadrupolar strength per cavity. (b) Ratio of surface peak fields. The effective longitudinal (c) and transverse (d) impedance for a whole system to provide the values in Table 1.

ISBN: 978-3-95450-191-5 doi:10.18429/JACoW-SRF2017-MOPB004

iris radius of $r_{\mathrm{ir}} = 60\,\mathrm{mm}$. This exceeds clearly the performance gain obtained by reentrant elliptical cavities.

The ratio of the surface peak f elds was throughout for all designs smaller than $2.13\,\mathrm{mT/(MV/m)}$ indicating a limitation by the electric f eld.

The effective longitudinal impedance of an entire system of four-vane cavities to satisfy the requirements in Table 1 is by a factor between two to four smaller than an adequate system of elliptical cavities provides. The effective transverse impedance is moderately larger but it is minor with respect to the LHC impedance budget.

LOMs and HOMs

Due to the large apertures at the ends of the cavity, only a few modes are trapped inside the cavity: a TE_{111}-like mode with a frequency between 700 and 750 MHz and a TM_{111}-like mode at around 1 GHz. The transverse wake spectrum is largely dominated by only the f rst dipole mode which can be easily extracted if the beam pipe radius becomes slightly larger by 20-30 mm. Based on this modif cation it is reasonable to apply LOM and HOM damping outside of the cryomodule using lossy materials in the beam pipe rather than couplers close to the cavity.

Multipole Fielderrors

These errors mainly arise from higher order multipoles b_m which satisfy the azimuthal periodicity of the fundamental multipole b_n (we have $n = 2$). They are correlated via the condition $m/n = 3, 5, 7, \ldots$ [10]. Table 4 shows the corresponding values of one optimized cavity.

Table 4: Different multipoles of the four-vane cavity with $r_{\mathrm{ir}} = 30\,\mathrm{mm}$ and $\alpha_{\mathrm{tap}} = 30\,\mathrm{deg}$

Multipole	Unit	Value for $E_{pk} = 50\,\mathrm{MV/m}$
b_2	$[\mathrm{Tm/m}]$	3.47×10^{-1}
b_6	$[\mathrm{Tm^5/m}]$	9.62×10^{4}
b_{10}	$[\mathrm{Tm^9/m}]$	1.98×10^{10}

The elliptical cavity do not provide any higher order multipoles due to the exact sinusoidal azimuthal dependency of the f eld components. However, there may appear so-called random multipole errors due to fabrication errors.

RF-Power

The optimal coupling for the fundamental mode coupler is derived from the input power required to compensate the beam loading assuming an off-centered beam. Fig. 11 shows the required input power for an optimized four-vane cavity as a function of the external quality factor for different transverse positions of the bunch. The needed input power is very moderate and by almost one order of magnitude smaller than required for the HL-LHC crab cavities [11], even for a bunch position as much as few mm from the cavity axis. This is only true if $Q_{\mathrm{ext}} > 1 \times 10^6$ can be used in operating the cavity.

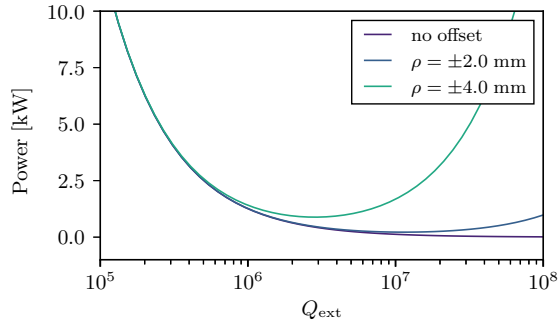

Figure 11: Input power as a function of the external quality factor for a four-vane cavity with an iris radius of $r_{\mathrm{ir}} = 30\,\mathrm{mm}$ and a tapering angle of $\alpha_{\mathrm{tap}} = 30\,\mathrm{deg}$. The beam offset is represented by the radial coordinate ρ. The bunch form factor F_{b} at 800 MHz is around 0.5 [12].

ACKNOWLEDGMENT

We especially acknowledge the fruitful discussions with Michael Schenk and Kevin Lee. The authors would also like to thank Rama Calaga, Slava Yakovlev, and Shahnam Gorgi Zadeh for their helpful recommendations.

REFERENCES

[1] A. Chao, *Physics of Collective Beam Instabilities in High Energy Accelerators*. Wiley-VCH Press, 1993.

[2] E. Métral *et al.,* Tech. Rep. CERN-ATS-2011-102, 2011.

[3] A. Grudiev, *Phys. Rev. ST Accel. Beams*, vol. 17, pp. 011001, Jan. 2014.

[4] L. R. C arver *et al.,* Tech. Rep. CERN-ACC-NOTE-2017-0012, 2017.

[5] J. Barranco García *et al., Phys. Rev. Accel. Beams*, vol. 19, pp. 101003, Oct. 2016.

[6] M. Schenk *et al.,* Tech. Rep. CERN-ACC-2016-0096, 2016.

[7] B. Aune *et al., Phys. Rev. ST Accel. Beams,* vol. 3, pp. 092001, Sep. 2000.

[8] F. Ruggiero, Tech. Rep. CERN-SL-95-09-AP, CERN, 1995.

[9] D. G. Myakishev and V. P. Yakovlev in *Proc. PAC*, vol. 4, (Dallas, USA), pp. 2348–2350 vol.4, May 1995.

[10] A. Wolski, *Beam dynamics in high energy particle accelerators*. London: Imperial College Press, 2014.

[11] R. Calaga, "Crab Cavities for the LHC Upgrade." presented at the Workshop on LHC Performance, Chamonix, 2012.

[12] J. Tückmantel Tech. Rep. CERN-ATS-Note-2011-002 TECH, CERN, 2010.